

Can an organoid recapitulate the metabolome of its parent tissue? A pilot NMR spectroscopy study

Abstract

Organoids are three-dimensional organ buds that are grown via stem cell cultivation and successfully recapitulate the microanatomy of the organs from which they are derived. They demonstrate excellent potential to study development, infectious disease, signaling pathways, drug toxicity, and the efficacy of various therapeutic agents. While it is known that organoids recapture organ microanatomy, how well they mimic organ function is currently unknown. Since metabolism is a downstream effect relative to genomics, transcriptomics, and proteomics, we have employed high-resolution ¹H NMR spectroscopy to observe the water-soluble metabolome and quantify how well organoids represent normal organ metabolism in two organoid-organ systems: the small intestine and the pancreas. This study shows that metabolism is significantly downregulated in the organoids relative to their respective organ system. Pronounced downregulation (~ an order of magnitude in organ-to-organoid concentration ratio) is observed in both the creatinine catabolic pathway and the choline pathway. Our conclusion is that organoids do not accurately recapitulate the metabolism of the organs from which they are derived. Appreciable modifications to the organoid cultivation process are needed if organoids are to realize their full potential in studying the functional properties of the organs they mimic and preemptively assessing an organ's response to therapy.

Keywords: Organoids; NMR; Metabolomics; Spectroscopy; Pancreas; Intestine; Metabolic recapitulation

Volume 8 Issue 7 - 2017

Joseph Weygand,² Sarah E Carter,¹ Travis C Salzillo,¹ Micheline Moussalli,¹ Bingbing Dai,^{1,2} Prasanta Dutta,¹ Xiangsheng Zuo,^{1,2} Jason B Fleming,³ Imad Shureiqi,⁴ Pratip Bhattacharya³

¹Department of Cancer Systems Imaging, The University of Texas MD Anderson Cancer Center, USA

²Graduate School of Biomedical Sciences, The University of Texas Health Science Center, USA

³Department of Pathology, The University of Texas MD Anderson Cancer Center, USA

⁴Department of Thoracic and Cardiovascular Surgery, The University of Texas MD Anderson Cancer Center, USA

⁵Department of Gastrointestinal (GI) Medical Oncology, The University of Texas MD Anderson Cancer Center, USA

⁶Department of Surgical Oncology, The University of Texas MD Anderson Cancer Center, USA

Correspondence: Pratip Bhattacharya, Associate Professor, Department of Cancer Systems Imaging, The University of Texas MD Anderson Cancer Center, 1881 East Road, Unit 1907, 3SCR4.3634, Houston TX 77054, USA, Tel 713-745-0769, Email pkbhattacharya@manderson.org

Received: December 15, 2017 | **Published:** December 21, 2017

Introduction

Organoids are stem cell-derived three-dimensional cellular clusters that serve as *in vitro* surrogates to an entire organ or organ segment. Organoids have successfully been cultured from various mouse and human stem cells, including embryonic stem cells (ESCs), induced pluripotent stem cells (iPSCs), and adult primary tissue.¹⁻³ Their self-assembled morphological structure and heterogeneous cellular composition mimic that of *in vivo* tissues and set it apart from flat homogenous cell lines.³⁻⁴ These unique morphological and cellular properties make organoids an excellent model to study development, infectious disease, and signaling pathways.⁵ For example, human cerebral organoids have been investigated as a potential model for neurodevelopment.⁶ There is also significant interest in utilizing human liver and kidney organoids in drug toxicity testing, where roughly 90% of drugs that pass the current rat toxicity model ultimately fail in clinical trials.⁷⁻⁸ Therapeutically, organoids could be used to grow new organs from a patient's own cells for transplantation or to evaluate possible treatment strategies by testing organoids derived from patient tissues.³ Indeed, personalized gut organoids from cystic fibrosis patients have been used to screen potential drugs, and liver buds have successfully been used to correct toxic liver failure in mice.⁹⁻¹⁰

Additionally, tumor organoids, or tumoroids, are proving to be valuable personalized medicine and cancer research tools. Unlike other surrogate model systems, such as patient-derived xenografts (PDXs), cancer cell lines, and three-dimensional tumor spheroids,

tumoroids retain tumor genetic heterogeneity and histopathology, as well as being less labor intensive and more time sensitive than other model systems.¹¹ Additionally, patient-derived tumoroids can be stored and expanded in organoid biobanks, which can then be utilized to identify novel therapies via high-throughput drug screens.¹¹⁻¹² Indeed, a proof-of-concept study showed the viability of organoid-based high-throughput drug screening by accurately predicting expected genotype-drug interactions in colorectal carcinoma (CRC) organoids.¹² Besides serving as patient surrogates, tumoroids have also been utilized as model systems to investigate tumorigenesis and the tumor microenvironment. For example, glioblastoma tumoroids have been developed to further elucidate influences on the tumor microenvironment, and CRC organoids have been used to investigate the role of niche dependency in tumor progression.¹³⁻¹⁴

While the morphological, genetic, and transcriptional similarities between organoids and their respective organs have been investigated, the metabolomics have not.^{7,15} Utilizing the fact that nuclei in different chemical environments resonate at different frequencies in the presence of an external magnetic field¹⁶, one can apply nuclear magnetic resonance (NMR) to interrogate tissue metabolism.¹⁷⁻¹⁸ In this study, high-resolution proton (¹H) NMR spectroscopy was employed to investigate the water-soluble metabolome of two murine-based organoid systems: the small intestine and the pancreas. We demonstrate that metabolism is significantly downregulated in both organoid systems relative to the organs from which they are derived, especially the creatine and choline catabolic pathways.

Materials and methods

Organoid cultivation

Murine *APC-CDX2-Cre*¹⁹ small intestines were opened longitudinally, washed with cold phosphate-buffered saline several times, cut into small pieces, transferred into 15 ml tubes with 5 mL of 10 mM ethylenediaminetetraacetic acid (EDTA) in chelation buffer (5.6 mM Na₂HPO₄, 8.0 mM KH₂PO₄, 96.2 mM NaCl, 1.6 mM KCl, 43.4 mM sucrose, 54.9 mM D-sorbitol, 0.5 mM DL-dithiothreitol), and left at room temperature for 10 minutes. The EDTA solution was removed, and chelation buffer was added. The tube was then shaken vigorously to isolate the intestinal crypts. Fragments were left to settle under normal gravity on ice for one minute, and the supernatant containing intestinal crypts was collected in a 50 mL tube coated with fetal bovine serum (FBS). The process of suspension and sedimentation was repeated 5–7 times and then all of the collected crypts were centrifuged for three minutes at 200 times the force of gravity. The pellet was resuspended in media and growth factor reduced matrigel (ratio: 1:3), plated in 24-well plates, and placed in a 37°C incubator for ten minutes to solidify the matrigel. Lastly, 500 µL of media was added (Advanced Dulbecco's Modified Eagle Media (DMEM)/F12 supplemented with 10 mM 4-(2-hydroxyethyl)-1-piperazineethanesulfonic acid (HEPES), Glutamax, penicillin/streptomycin, 1x N2, 1X B27, 1 mM N-Acetylcysteine) which contained the following growth factor combination: murine epidermal growth factor (EGF) 50 ng/mL, murine Noggin 100 ng/mL, and human R-spondin-11 µg/mL.¹⁵

BALB/c-nu/j mice (Jackson Laboratory, Bar Harbor, ME) were euthanized and murine pancreases harvested. One-third of the pancreatic tissue was flash-frozen and stored at -80°C, with the rest used for pancreatic ductal isolation and organoid culture using reported methods.^{20–22} Briefly, pancreatic tissue was minced with a scalper and digested with 0.012% collagenase XI (w/v) (Sigma), dispase 0.012% (w/v) (Gibco), and FBS (Gibco) 1% in DMEM media (Gibco) at 37°C for 2 hours. Digested pancreatic tissue was washed with DMEM four times. Pancreatic ducts were manually chosen with a P20 Pipetmen under a microscope. Isolated ducts were mixed with 50 µl growth factor reduced Matrigel (BD Bioscience) and seeded in a 24-well plate. Advanced DMEM/F12 culture medium was added upon Matrigel solidification. The culture media was prepared with Advanced DMEM/F12 (Invitrogen) supplemented with 10 nM gastrin (Sigma), 1.25 mM N-Acetylcysteine (Sigma), B27 (Invitrogen), 50 ng/ml EGF (Peprotech), 100 ng/ml fibroblast growth factor 10 (FGF10) (Peprotech), 10 mM Nicotinamide (Sigma), and 10% Wnt-3a, R-spondin-3 (RSPO3), and Noggin-conditioned media (v/v), which were prepared with the cell line L-WRN (ATCC) using reported methods.²³ About one week after seeding, organoids were dissociated into small fragments for passage or frozen stock.

NMR spectroscopy

Each sample was weighed, crushed, and immersed in 3 mL of methanol-to-water mixture (2:1) (UHPLC grade water (Optima, Thermo Fisher Scientific)) on top of 0.5 mL of polymer vortex beads inside a 15 mL test tube. A process of mechanical homogenization was performed by vortexing the tubes for 15 seconds, flash-freezing in liquid nitrogen for one minute, and allowing the mixture to thaw, repeated three times. The samples were then subjected to centrifugation for ten minutes to separate the water-soluble metabolites from the proteins and other cellular constituents. The supernatant was extracted and subjected to rotary evaporation to remove the methanol. The samples were further desiccated by placing them on a lyophilizer

overnight. The metabolites were then reconstituted in a solution of 600 µL of deuterated water (D₂O), 36 µL of phosphate buffer, and 4 µL of 80 mM DSS-d₆ (3-trimethylsilyl-1-propanesulfonic acid-d₆ sodium salt). The phosphate buffer was added to stabilize any potential pH variations, and the DSS-d₆ served as the reference standard by which the spectral signal could be normalized for each metabolite.

¹H NMR spectroscopy was performed on a Bruker AVANCE III HD[®] NMR scanner (Bruker Bio Spin Corporation, The Woodlands, TX) equipped with a Prodigy BBO cryoprobe at a temperature of 298 K. The cryoprobe increases the sensitivity of the measurement three to four fold. All supplies (D₂O, DSS-d₆, phosphate buffer) were purchased from Sigma Aldrich without further purification. The spectrometer operates at a ¹H resonance frequency of 500 MHz and is endowed with a triple resonance (¹H, ¹³C, ¹⁵N) cryogenic temperature probe with a Z-axis shielded gradient. A pre-saturation technique was implemented for water suppression. The spectra were obtained with a 90° pulse width, a scan delay t_{rel} of 6.0 s, a 10240 Hz spectral width, and an acquisition time t_{max} of 1.09 s (16,000 complex points). A total of 256 scans were collected and averaged for each spectrum, which resulted in a total scan time of 32 minutes and 49 seconds. Here, $t_{rel} + t_{max}$ was nearly 8 s so that it was greater than $3 \cdot T_1$ of the metabolites observed.²⁴ The time domain signal was apodized using an exponential function. A total of 17 one-dimensional ¹H spectra were acquired, of which 6 were small intestinal organoids, 5 were small intestinal tissue, 3 were pancreatic organoids, and 3 were pancreatic tissue.

After the spectra were acquired, metabolic profiling was performed in Chenomx NMR Suite 8.1 software (Chenomx Inc., Edmonton, Canada). Quantification of the metabolites was then performed using MestReNova software (Mestrelab Research, Santiago, Spain) by integrating some nonzero region centered about the chemical shift at which the metabolite is known to resonate. Integrated values of metabolites were determined by taking the ratio of the resonance for each metabolite over the DSS-d₆ resonance. Metabolite resonances were identified through reference to either of two online metabolomics databases, Human Metabolome Database (<http://www.hmdb.ca>) or Biological Magnetic Resonance Bank (<http://www.bmr.b.wisc.edu/metabolomics>). Since NMR signal is directly proportional to the amount of material in the test tube, this value is further normalized by the mass obtained prior to immersion in methanol-to-water mixture. Prior to integration, phase and baseline corrections were performed manually in MestReNova.

Statistical methods

To determine whether statistical significance was achieved, we performed an unpaired, two-sample, two-tailed t-test with equal variance.²⁵ Significance was achieved if the p-value $\alpha < 0.05$.

Results

Figure 1 illustrates representative spectra obtained from ¹H NMR metabolomics of the small intestinal crypt versus small intestinal organoid system. An example spectrum obtained from normal small intestinal tissue is shown in Figure 1A and a spectrum obtained from a small intestinal organoid is shown in Figure 1B. In both organ systems studied (small intestine and pancreas), the normal tissue exhibits overall higher baseline metabolic activity than the organoids. This is especially true for the metabolites involved in both the creatinine catabolic pathway and the choline pathway.

Figure 2 depicts relative concentration of metabolites involved in the creatinine catabolic pathway for the normal tissue (blue) and organoids (red) for both the small intestinal system (Figure 2A) and

the pancreatic system (Figure 2B). There is 8.6 times more creatine in small intestinal tissue than small intestinal organoids and 5.1 times more creatine in pancreatic tissue than pancreatic organoids, achieving p-values of $\alpha = 0.0013$ and $\alpha = 0.022$, respectively. Similarly, there is 8.7 times more glycine in small intestinal tissue than small intestinal organoids and 13.4 times more glycine in pancreatic tissue than pancreatic organoids, achieving p-values of $\alpha = 0.0046$ and $\alpha = 0.00051$, respectively.

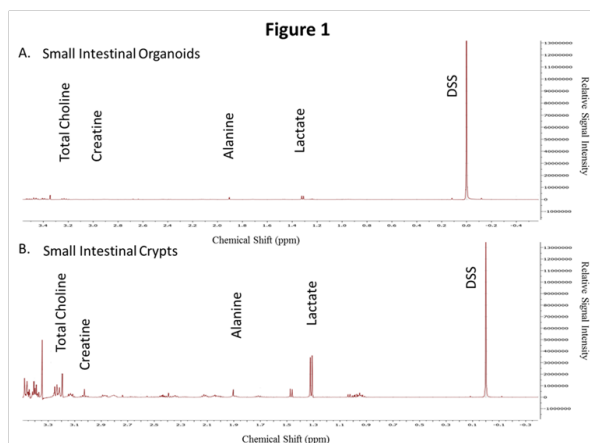


Figure 1 Representative NMR spectra. Here representative NMR spectra of small intestinal organoids (A.) and small intestinal crypts (B.) are shown. Relative signal intensity is depicted on the vertical axis, and chemical shift is depicted on the horizontal axis. Some common metabolites are indicated at their appropriate chemical shifts. DSS-d6 (3-trimethylsilyl-1-propanesulfonic acid-d6 sodium salt) is the reference standard added to system to which each metabolite concentration is normalized.

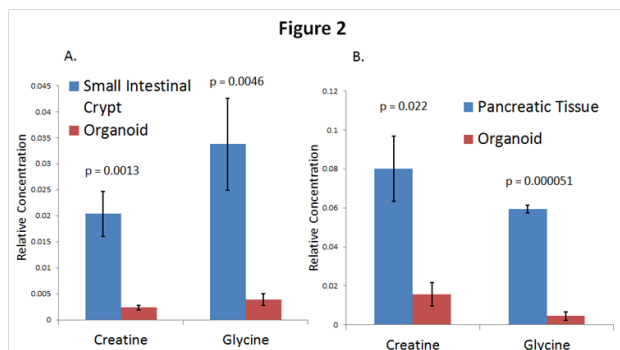


Figure 2 Relative concentration of metabolites in the creatinine catabolic pathway. Creatine and glycine are both significantly downregulated in organoids relative to the normal tissue from which they derive. This is shown in both the small intestine (A.) and the pancreas (B.)

Figure 3 illustrates relative concentration of metabolites involved in the choline pathway for the normal tissue (blue) and organoids (red) for both the small intestinal system (Figure 3A) and the pancreatic system (Figure 3B). Here, total choline is defined as the sum of the three adjacent integrals over choline, phosphocholine, and glycerophosphocholine. There is 12.9 times more choline in small intestinal tissue than small intestinal organoids and 44.7 times more choline in pancreatic tissue than pancreatic organoids, achieving p-values of $\alpha = 0.0011$ and $\alpha = 0.0077$, respectively. Also, there is 9.8 times more total choline in small intestinal tissue than small intestinal organoids and 7.4 times more total choline in pancreatic tissue than pancreatic organoids, achieving p-values of $\alpha = 0.00047$ and $\alpha = 0.0064$, respectively.

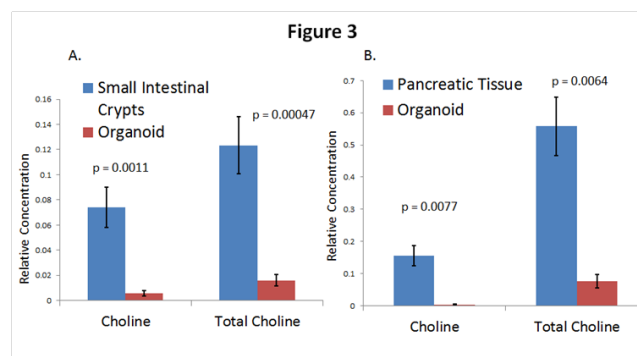


Figure 3 Relative concentration of metabolites in the choline pathway. The choline pathway is significantly downregulated in organoids relative to the normal tissue from which they derive. This is shown in both the small intestine (A.) and the pancreas (B.). Here, the relative concentration of total choline is determined by integrating the three consecutive peaks: choline, phosphocholine, and sn-glycero-3-Phosphocholine prior to normalization.

In addition, we also observed significantly higher glutamate concentration in tissue relative to organoids in both the small intestinal system ($\alpha = 0.0015$) and the pancreatic system ($\alpha = 0.0021$). There was also more lactate in the tissue relative to organoids in both systems, but, while statistical significance was only barely achieved in the small intestinal system ($\alpha = 0.046$), it was not achieved in the pancreatic system ($\alpha = 0.31$). Lastly, we observed significantly higher alanine concentration in tissue relative to organoids in both the small intestinal system ($\alpha = 0.016$) and the pancreatic system ($\alpha = 0.0035$). All other metabolite pools that were identified and quantified had either insignificantly higher concentration in the organs, insignificantly higher concentrations in the organoids, or roughly equal concentrations in both systems.

Discussion

Overall there was less metabolic activity in the organoids than in the organ tissue (Figure 1). Isolated from the rest of the body and the complex cell-to-cell signaling including growth factors, hormones, etc., which are so intimately involved with regulating a cell's metabolic functioning, it is not surprising that there are metabolic differences between *in vitro* organoids and *in vivo* tissue. Possible explanations for the most striking and significant of the differences, particularly in the creatine and choline pathways and in nonessential amino acid metabolism, are addressed below, although further research is required to truly elucidate the cause of these observed metabolic differences and develop a mechanistic understanding.

The creatinine catabolic pathway exhibited significant variation between the organoids and the intestinal tissue, with 8.6 and 8.7 times more creatine and glycine in the organ tissue, respectively (Figure 2A). The creatine cycle is intimately involved in the storage and release of energy, especially in organs with high energy consumption such as the brain or muscle.²⁶ The creatine transporter (CRT) exists on the outside of intestinal cells and is responsible for absorbing creatine from food sources as it enters the intestinal tract.²⁷ Therefore, it is possible that the small intestinal organoid, isolated from the rest of the body and digestive tract, was severed from its main source of creatine leading to the observed difference in creatine and glycine levels. This, however, does not explain why the pancreas organoid versus pancreas tissue data yielded a similar metabolic discrepancy, with the organoid having 5.1 times less creatine and 12.4 times less glycine than the tissue (Figure 2B). The pancreas, unlike the small intestine,

procures most of its creatine through synthesis of amino acids using enzymes such as the arginine:glycine aminotransferase (AGAT).²⁸ Thus, explanations for the low levels of creatine and glycine could be attributed to differences in the genetic and transcriptional basis surrounding the enzymatic function of aminotransferases such as AGAT in the pancreas. Regardless, further investigation into the underlying interconnected crosstalk between genetic, transcriptional, and translational factors concerning key proteins in creatinine catabolism such as CRT and AGAT is required to fully elucidate the biological causes of the observed low concentrations of creatine and glycine in pancreatic and intestinal organoids and beyond the scope of this NMR spectroscopy based study.

There was also a large and significant difference in the total choline levels in both the intestinal and pancreatic organoids and tissues, with 9.8 times less total choline in the intestinal organoids versus the intestine and 7.4 times less in the pancreatic organoids versus the pancreas (Figure 3). Choline metabolism in the small intestine is intricately involved with bacteria in the microbiome which conduct anaerobic processing of choline to produce trimethylamine (TMA), acetate, and ethanol.²⁹ The metabolic discrepancy therefore could arise from the organoid culturing technique, where the organoid, unlike its tissue counterpart, exists entirely separate from the microbiome and subjected to antibiotics. In the case of the pancreas organoids, previous investigations have shown that choline concentrations are extremely sensitive to oxygen levels; it has been theorized that hypoxic conditions lead to increased breakdown of phospholipids and therefore increased levels of choline and phosphocholine.³⁰ Without the protective hypoxic environment of the pancreas and surrounding bodily tissues, the total choline levels in the organoids would decrease. Regardless, further investigation is required to investigate choline differences between organoid and tissue and identify possible explanations.

Glutamate was found in significantly lower concentrations in the organoids relative to their respective tissues. In particular, there was 6.6 times more glutamate in the intestinal tissue than in the intestinal organoids and 8.3 times more glutamate in the pancreatic tissue than in the pancreatic organoids. Glutamate serves as an important oxidative fuel for the intestine, as, in addition to the liver, the intestine is a major site of glutamate and amino acid catabolism.³¹ The intestinal organoids would acquire glutamate via the metabolic conversion of the essential amino acids present in supplemented culture media, which differs in nutrient content from the mouse diet processed by the *in vivo* intestinal tissue. This difference in glutamate concentration in the intestine relative to the intestinal organoids could reflect the drastically different mechanisms and nutrient conditions through which glutamate was metabolized. Additionally, amino acid levels, including glutamate, were previously shown to be significantly decreased in the lower small intestinal lumen of germfree mice when compared to conventional mice.³² Large pools of undigested endogenous protein in germfree animals also suggest a critical role for the microbiome in the digestion of protein into amino acids and their subsequent absorption by surrounding tissues.³² Continuing research into complex microbial-host metabolic interactions further underscores the importance of the microbiome in amino acid synthesis, degradation, and overall homeostasis.³³ Thus, the lack of a microbe-intestinal homeostatic interface in the intestinal organoids could further explain the lower levels of glutamate *in vitro* versus *in vivo*. In the pancreas, glutamate alters the viability and function of the endocrine cells in pancreatic islets.³⁴ However, the organoids in this study are derived from pancreatic ductal cells. The pancreatic duct, which is responsible for supplying the common bile duct with pancreatic juice, is not involved in the endocrine function of

the pancreas. This physiological difference could account for lower concentrations of glutamate in the ductal organoids than in the pancreas as a whole.

Finally, alanine was found to be significantly downregulated in the organoids relative to their respective tissues, as the concentration of alanine was 2.9 times greater in intestinal tissue than in intestinal organoids and 7.3 times greater in pancreatic tissue than in pancreatic organoids. Alanine, like glutamate, is a nonessential amino acid, and thus the observed differences in alanine concentration could also be explained by the aforementioned divergence in the mechanisms by which nutrients are provided *in vitro* versus *in vivo*. Additionally, as was also mentioned previously in relationship to glutamate concentrations, alanine has also been shown to exist at decreased levels in the lumen of the lower small intestine in germfree mice than in mice with functioning microbiomes.³² In the pancreas, high levels of circulating amino acids after a protein-rich meal can stimulate the release of insulin and glucagon.³⁵ Furthermore, it has been shown that alanine is found in greater concentrations in the pancreatic islet cells in mice³⁶, suggesting that alanine, like glutamate, contributes more to the endocrine function of the pancreas. Since the pancreatic organoids studied here derive from the ductal cells, it is not surprising that one observes significantly downregulated alanine levels relative to pancreatic tissue.

Conclusion

As this investigation into the metabolome of organoids versus the model organ suggests, there is still much work to be done to fully perfect the organoid as a tool in drug development, precision medicine, and biomedical research. This research described underscores the importance of metabolism in organoid research to understand the functional properties of the organs they mimic. Through further studies, the source of this metabolic discrepancy between organoids and organs will become apparent, and corrections will be made to make organoids precisely recapitulate the metabolism of the *in vivo* tissue. Perhaps small corrections in the timing, amount, and type of growth factors, which are intimately involved with the proper function of metabolic pathways, will prove the modification needed to make organoids more metabolically viable. Either way, the results of this study and further studies into organoid metabolomics will surely contribute to the growing story of organoids by adding the metabolic tale to the transcriptional, genetic, and morphological canon.

Acknowledgements

We would like to thank the CCSG-funded small animal imaging facility and NMR facility (CA016672) at M.D. Anderson Cancer Center. Funding: We also thank Koch Foundation, NCI R25R21CA185536-02, CPRIT- RP150701, MD Anderson IRG grants, MD Anderson Moonshot funding MD Anderson summer research fellowship and MD Anderson startup for funding support.

Conflicts of interest

The authors declare that they have no conflict of interests.

Funding

None.

References

1. Lancaster MA, Knoblich JA. Organogenesis in a dish: Modeling development and disease using organoid technologies. *Science*. 2014;345(6194):1247125.

2. Willyard C. The boom in mini stomachs, brains, breasts, kidneys and more. *Nature*. 2015;523(7562):520–522.
3. Fatehullah A, Tan SH, Barker N. Organoids as an *in vitro* model of human development and disease. *Nat Cell Biol*. 2016;18(3):246–254.
4. Sasai Y, Eiraku M, Suga H. *In vitro* organogenesis in three dimensions: self-organising stem cells. *Development*. 2012;139(22):4111–4121.
5. McCracken KW, Catá EM, Crawford CM, et al. Modelling human development and disease in pluripotent stem-cell-derived gastric organoids. *Nature*. 2014;516(7531):400–404.
6. Camp JG, Badsha F, Florio M, et al. Human cerebral organoids recapitulate gene expression programs of fetal neocortex development. *Proc Natl Acad Sci U S A*. 2015;112(51):15672–15677.
7. Shanks N, Greek R, Greek J. Are animal models predictive for humans? *Philos Ethics Humanit Med*. 2009;4(1):1–20.
8. Akhtar A (2015) The flaws and human harms of animal experimentation. *Camb Q Healthc Ethics* 24: 407–419.
9. Dekkers JF, Berkers G, Kruisselbrink E, et al. Characterizing responses to CFTR-modulating drugs using rectal organoids derived from subjects with cystic fibrosis. *Sci Transl Med*. 2016;8(344):1–13.
10. Takebe T, Sekine K, Enomura M, et al. Vascularized and functional human liver from an iPSC-derived organ bud transplant. *Nature*. 2013;499(7459):481–484.
11. Shroyer NF. Tumor organoids fill the niche. *Cell Stem Cell*. 2016;18(6):686–687.
12. van de Wetering M, Francies HE, Francis JM, et al. Prospective derivation of a living organoid biobank of colorectal cancer patients. *Cell*. 2015;161(4):933–945.
13. Hubert CG, Rivera M, Spangler LC, et al. A three-dimensional organoid culture system derived from human glioblastomas recapitulates the hypoxic gradients and cancer stem cell heterogeneity of tumors found *in vivo*. *Cancer Res*. 2016;76(8):2465–2477.
14. Fujii M, Shimokawa M, Date S, et al. A colorectal tumor organoid library demonstrates progressive loss of niche factor requirements during tumorigenesis. *Cell Stem Cell*. 2016;18(6):827–838.
15. Sato T, Vries RG, Snippert HJ, et al. Single Lgr5 stem cells build crypt-villus structures *in vitro* without a mesenchymal niche. *Nature*. 2009;459(7244):262–265.
16. Weygand J, Fuller CD, Ibbott GS, et al. Spatial precision in magnetic resonance imaging-guided radiation therapy: The role of geometric distortion. *Int J Radiat Oncol Biol Phys*. 2016;95(4):1304–1316.
17. Salzillo TC, Hu J, Nguyen L, et al. Interrogating metabolism in brain cancer. *Magnetic Resonance Imaging Clinics*. 2016;24(4):687–703.
18. Wang J, Weygand J, Hwang KP, et al. Magnetic resonance imaging of glucose uptake and metabolism in patients with head and neck cancer. *Sci Rep*. 2016;6:30618.
19. Grivnikov SI, Wang K, Mucida D, et al. Adenoma-linked barrier defects and microbial products drive IL-23/IL-17-mediated tumour growth. *Nature*. 2012;491(7423):254–258.
20. Huch M, Bonfanti P, Boj SF, et al. Unlimited *in vitro* expansion of adult bi-potent pancreas progenitors through the Lgr5/R-spondin axis. *The EMBO J*. 2013;32(20):2708–2721.
21. Boj SF, Hwang C-I, Baker LA, et al. Organoid models of human and mouse ductal pancreatic cancer. *Cell*. 2015;160(1–2):324–338.
22. Broutier L, Andersson-Rolf A, Hindley CJ, et al. Culture and establishment of self-renewing human and mouse adult liver and pancreas 3D organoids and their genetic manipulation. *Nat Protoc*. 2016;11(9):1724–1743.
23. Miyoshi H, Stappenbeck TS. *In vitro* expansion and genetic modification of gastrointestinal stem cells in spheroid culture. *Nat Protoc*. 2013;8(12):2471–2482.
24. Pudakalakatti SM, Uppangala S, D'Souza F, et al. NMR studies of preimplantation embryo metabolism in human assisted reproductive techniques: A new biomarker for assessment of embryo implantation potential. *NMR in Biomedicine*. 2013;26(1):20–27.
25. De Muth JE. Overview of biostatistics used in clinical research. *Am J Health Syst Pharm*. 2009;66(1):70–81.
26. Joncquel-Chevalier Curt M, Voicu P-M, Fontaine M, et al. Creatine biosynthesis and transport in health and disease. *Biochimie*. 2015;119:146–165.
27. Peral MJ, García-Delgado M, Calonge ML, et al. Human, rat and chicken small intestinal Na⁺ – Cl[–] – creatine transporter: functional, molecular characterization and localization. *The Journal of Physiology*. 2002;545(1):133–144.
28. da Silva RP, Clow K, Brosnan JT, et al. Synthesis of guanidinoacetate and creatine from amino acids by rat pancreas. *Br J Nutr*. 2014;111(4):571–577.
29. Bressenot A, Pooya S, Bossenmeyer-Pourie C, et al. Methyl donor deficiency affects small-intestinal differentiation and barrier function in rats. *British Journal of Nutrition*. 2013;109(4):667–677.
30. Long RC, Papas KK, Sambanis A. *In vitro* monitoring of total choline levels in a bioartificial pancreas: ¹H NMR spectroscopic studies of the effects of oxygen level. *Journal of Magnetic Resonance*. 2000;146(1):49–57.
31. Burrin DG, Stoll B. Metabolic fate and function of dietary glutamate in the gut. *Am J Clin Nutr*. 2009;90(3):850S–856S.
32. Whitt DD, Demoss RD. Effect of microflora on the free amino acid distribution in various regions of the mouse gastrointestinal tract. *Appl Microbiol*. 1975;30(4):609–615.
33. Neis EPJG, Dejong CHC, Rensen SS. The role of microbial amino acid metabolism in host metabolism. *Nutrients*. 2015;7(4):2930–2946.
34. Otter S, Lammert E. Exciting times for pancreatic islets: glutamate signaling in endocrine cells. *Trends Endocrinol Metab*. 2016;27(3):177–188.
35. Schmid R, Schusdziarra V, Schulte-Frohlinde E, et al. Circulating amino acids and pancreatic endocrine function after ingestion of a protein-rich meal in obese subjects. *The Journal of Clinical Endocrinology & Metabolism*. 1989;68(6):1106–1110.
36. Hellman B, Sehlin J, Täljedal IB. Uptake of Alanine, Arginine, and Leucine by Mammalian Pancreatic β -Cells. *Endocrinology*. 1971;89(6):1432–1439.